Mechanical Characterization of Composite Solid Propellants

G.B. Brunella, G. Sandri Tussiwand*, F. Maggi*, S. Cerri*, L.T. DeLuca*, L. Galfetti*, B. D'Andrea***
**SPLab, Dipartimento di Energetica, Politecnico di Milano, I – 20156 Milan, Italy*
***Avio S.p.A., I-00034 Colleferro, Rome, Italy*

Abstract

An extensive mechanical characterization for a series of AP/HTPB-based propellants was performed. Mechanical properties are correlated to propellant composition, showing the effects of the ammonium perchlorate grain size distribution and bonding agent. Due to the importance of damage and fracture propagation with respect to the behavior of a solid rocket motor, fracture mechanics and crack propagation properties were also tested. Tensile tests of cracked MT specimens were performed at three displacement rates to measure the material's toughness. Three different geometries were tested to investigate the effect of the specimen thickness on toughness. Moreover, the work was extended to measure the burning rate of material samples under strain application.

Nomenclature

A_0 = initial sample section, mm^2
AP = Ammonium Perchlorate
D = nominal particle size, μm
$E_{5\%}$ = equivalent propellant stiffness, N mm^{-2} in the elastic region (before the onset of damage)
F = applied load, N
HTPB = Hydroxyl-Terminated Polybutadiene
K_I = Stress Intensity Factor
K_{IC} = toughness (critical stress intensity factor)
L_0 = initial sample length, mm
MT = Middle Tension Panel
SIF = Stress Intensity Factor
SRM = Solid Rocket Motors
U = strain energy, mJ mm^{-3}
U_{break} = rupture energy strain, mJ mm^{-3}
ΔL = sample variation, $L-L_0$, mm
υ = Poisson ratio
σ_{corr} = corrected stress, N mm^{-2}
σ_{eng} = engineering stress, N mm^{-2}
ε_{lin} = linear strain
ε_{log} = logarithmic strain
$\langle\rho\rangle$ = density, g cm^{-3}
$d\varepsilon/dt$ = strain rate, mm min^{-1}

1. Introduction

Metals and different oxidizer grain sizes are inserted into propellant formulations in order to increase their ballistic performance, density and packing volume (the latter increases both the volumetric specific impulse and the specific impulse itself, reducing the mass average diameter of the agglomerates resulting from combustion).
The oxidizer grains distribution and crystals average diameter affect the mechanical and balistic properties of a propellant; this has relevant effects on the structural integrity of a motor, since the propellant failure properties determine its safety under a given mechanical load, and an insufficient modulus can lead to system failure through

excessive grain deformation and structural-ballistic interaction (e.g. as in the Titan IV SRMU prequalification test failure on the 1st of April 1991[1]). Several mechanisms can lead to the motor's failure: the detachment of propellant fragments can occlude the bore or the nozzle and cause a case burst. Moreover, the presence of flaws and growing cracks into the grain is dangerous , affecting safety or reliability: if the flame propagates within a crack or flaw it can cause a burning surface evolution potentially very different from expectations, leading to the burst of the case either through excessive pressure, or through a burn-through.
Composite propellants are heterogeneous materials with a high percentage of solid particles of irregular shape (85-90 wt. percent). Therefore, the presence of defects and cracks is very likely. In order to predict the state of stress and strain on the material, generated by the loads acting on the motor, one needs to characterize its mechanical behavior, simulate the grain response to defined input loads and introduce appropriate failure criteria to evaluate the motor safety at ignition. Often, mechanical and ballistic properties require opposite propellants characteristics, so a compromise is needed during chemical development. A complete propellant characterization requires both ballistic and mechanical tests.

Mechanically, propellants are non-linear, viscoelastic materials. Their response to an applied load depends on many factors: loading conditions (direction, intensity, and loading rate), boundary conditions (temperature, pressure, and humidity), and loading history. Thermoviscoelasticity is the main propellant characteristic: its stiffness depends on time and temperature; its behavior is quite similar to the one of other filled elastomers: it is stiffer if loaded quickly and/or exposed to low temperature, it is less stiff if loaded slowly and/or subjected to high temperature. Often, a linear thermoviscoelastic constitutive behavior is assumed to simplify structural analysis. In the last years, a NATO working group has identified specific parameters and test methods for the mechanical characterization of energetic materials[2]. Accordingly, mechanical tests are divided in two groups: tests to determine the constitutive properties (necessary to carry out a structural analysis) and tests to determine failure properties (in order to determine the margin of safety of a grain subjected to mechanical loads, including ignition).

This work is focused on the mechanical characterization of AP/HTPB-based propellants[3]. The first part of the paper shows the main characteristics of the formulations used in this study. Stiffness, rupture and fracture properties (tensile strength, strain at maximum stress, strain energy, and critical stress intensity factor, SIF), were investigated at different strain rates (0.5, 5, 50, and 500 mm/min) at room temperature. Fracture behavior was only characterized for two propellants. Results are presented in the second part and show the viscoelastic behavior of all materials. The third part stresses the importance of a fracture-mechanical investigation. Tensile tests of cracked samples were performed at three displacement rates. Furthermore three different specimen geometries were studied in order to investigate thickness and deformation rates effects as well. The last part comments the burning rate of propellant samples under load. Concluding remarks complete the paper.

2. Solid propellants formulation

The composite solid propellants tested in this study were industrially produced. The composition is proprietary but general characteristics are given in Table 1. Three propellants with the same ammonium perchlorate, aluminum and polymeric binder (AP/Al/HTPB) nominal composition, but different powder size and distribution, were investigated together with a common 68/18/14 propellant taken as reference formulation. All propellants contain bi or three-modal oxidizer grain distributions. Reference and D propellants are quite similar; propellants B and C differ only with respect to the amount of coarse AP (B contains a greater amount of 200 μm AP with respect to the content of 400 μm AP, and propellant C is the opposite). Density was measured through a MD200 densimeter.

Table 1 : AP grain size distribution and density

	Reference	**B**	**C**	**D**
AP size distribution	Fine[a], 200	Fine, 200, 400	Fine, 200, 400	Fine, 200
AP fine amount (qualitative)	High	Low	Medium	High
<ρ>	1.729	1.788	1.779	1.775

[a] Fine AP means AP particles size of about 10 μm.

3. Mechanical properties

A mechanical characterization of the propellants presented in Table 1 was carried out. Propellant specimens were tested through uniaxial tensile tests at constant strain rate[4]. During each test, the applied load and displacement were recorded. Knowing the specimen dimensions (length L, and section A) one obtains the stress-strain constitutive behavior, both in terms of nominal $\sigma(\varepsilon)$, or corrected σ and natural ε. Specimens were obtained from a propellant slab (thickness of 3-4 mm); samples and test procedures follow the standard STANAG 4506[4]. For each deformation rate a minimum of three samples were tested.

Dogbone samples (according to DIN 53 504 - S3A) of all propellants were tested at different strain rates: 5, 50, and 500 mm/min. Propellants B and C were also tested at 0.5 mm/min. Reference propellant and propellant D appear softer than the other ones (Figure 2). Propellant B is the hardest. Surface splintering phenomena were observed for propellant B and C; these behaviors were not observed for reference propellant and formulation D: formulations B and C easily lost coarse AP particles when the surface was rubbed, unlike with reference and D, possibly indicating a reduced bonding agent effectiveness. The thermoviscoelastic behavior was characterized in terms of corrected stress ($\sigma_{corr}=\sigma_{eng}(1+\varepsilon_{lin})$), and logarithmic strain ($\varepsilon_{log}=\log(1+\varepsilon_{lin})$). Therefore, for each propellants and strain rate $d\varepsilon/dt$, the average values of stiffness at 5% of strain, tensile strength and the corresponding strain were obtained. The rupture strain energy is also reported.

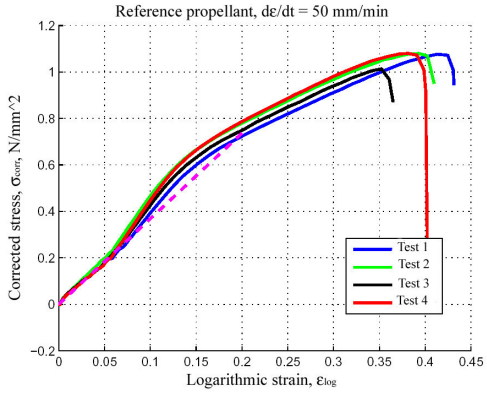

Figure 1 : Logarithmic strain and corrected stress for reference propellant at $d\varepsilon/dt$ = 50 mm/min

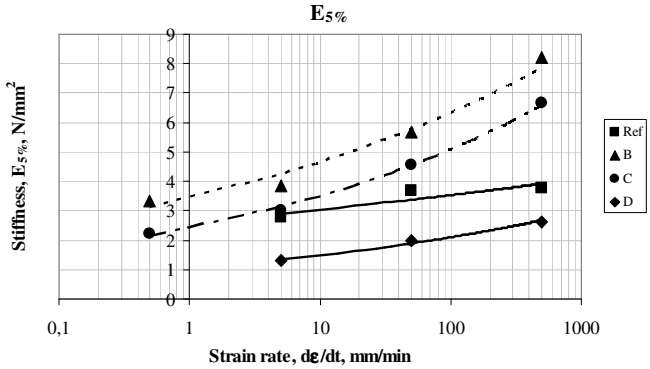

Figure 2 : Propellants stiffness ($E_{5\%}$) at different logarithmic strain rates

Figure 1 shows the typical mechanical behavior of reference propellant at $d\varepsilon/dt$=50 mm/min. Stress-strain curves show an initial linear part; after this initial step, the material presents strain hardening behavior and then a decreasing stiffness (softening) caused by damage. Values of stiffness ($E_{5\%}$) were obtained and the average value determined. For this material, a fourth test was necessary; the premature rupture in one case (test #3, Figure 1) was probably due to internal material defects. Stiffness increases with strain rate for each propellant; this is a typical trend for a viscoelastic material. Focusing the attention on Figure 2, it can be noted that propellants with similar formulation and AP distribution grains size show the same kind of trend with strain rate (reference propellant and propellant D; propellants B and C). B has the highest stiffness value, then follows C, Reference, and D (Figure 3). High stiffness values correspond to a reduced strain capability, as expected.

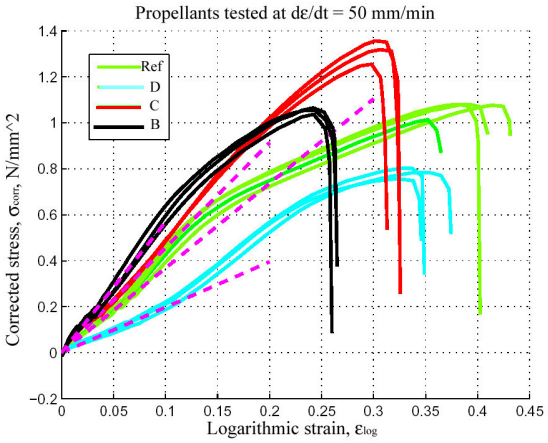

Figure 3 : Propellants tested at dε/dt = 50 mm/min

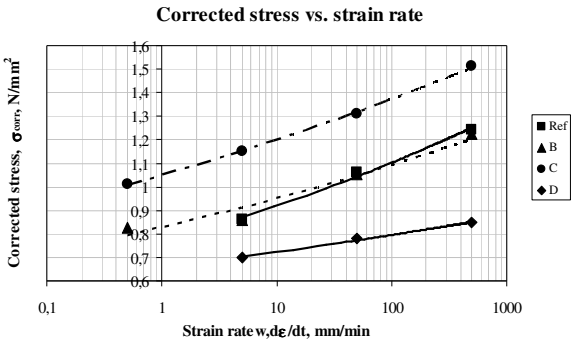

Figure 4 : Propellants corrected stress (σ_{corr}) at different logarithmic strain rates

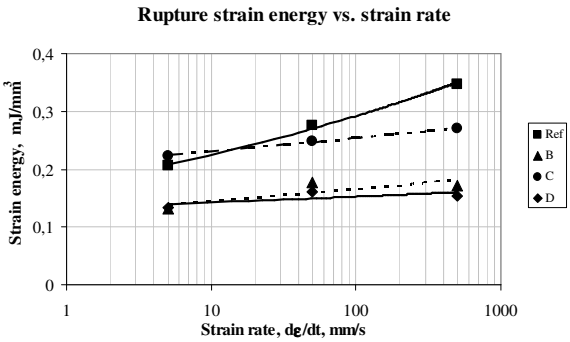

Figure 5 : Propellants rupture strain energy at different logarithmic strain rates

Propellants show increasing maximum corrected stress values with increasing strain rate. These are monotonic trends. Propellant C shows the highest maximum stress value, reference and B have the same strength in the range 5-500 mm/min. D shows reduced strength (Figure 4). Strain energy or strain energy density is another useful mechanical performance index for a propellant. A good energetic material has high rupture strain energy (U_{rupt}). In Figure 5, the rupture strain energies are reported. Between 5 and 50 mm/min all propellants show increasing energy values; then, at higher strain rates, only reference propellant and propellant C show growing strain energies.

4. Fracture mechanics

Only propellants B and C were tested to study the crack propagation behavior. These energetic materials contain a coarser oxidizer. Uniaxial tests show higher stiffness and lower rupture strain than reference propellant and propellant D. Middle tension panels (MT), prepared according to ASTM standard procedures[5], were tested through uniaxial tensile tests at constant strain rate, using the INSTRON experimental set-up shown in Figure 6. For every strain rate, a minimum of three specimens were tested. The toughness (K_{IC}) of the materials was determined at three different strain rates; thickness effects were also tested.

Table 2 : Middle tension panel geometry

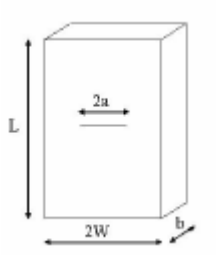

Geometry	L, mm	2W, mm	2a, mm	b, mm
A	68-71	30-32	15	5
B	68-71	30-32	15	7.5
C	68-71	30-32	15	10

For each test, load-displacements and stress-strain curves were obtained. Their analysis provides information about possible loading anomalies. Irregularities are directly related to non conventional crack propagation or to set-up problems. The thermoviscoelastic behavior of the energetic materials was characterized in terms of engineering stress ($\sigma_{eng}= F/A_0$) and linear strain ($\varepsilon_{lin}=\Delta L/L_0$). Necking of the cross-sectional area of the specimen is caused by two factors: longitudinal dilatation due to the propellant near incompressibility ($\upsilon \approx 0.5$), i.e. a reduction in the cross section, and mode I crack propagation; the latter represents the main contribute. An example of a stress-strain curve for propellant B is reported in Figure 7. Results show consistency and reproducibility; the ultimate tensile stress (or load) values, e.g. the parameters determining toughness, are sufficiently close to each other.

Figure 6 : INSTRON experimental set-up

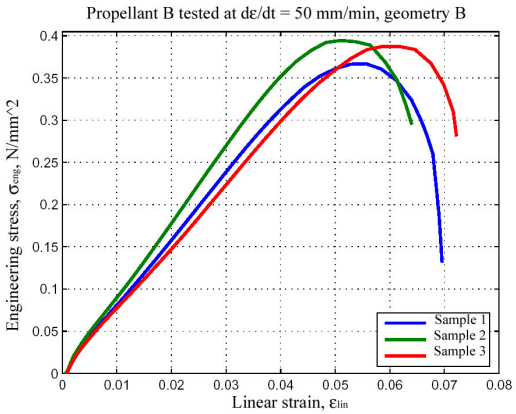

Figure 7 : Stress-strain curve (σ_{eng}-ε_{lin}) for propellant B, at dε/dt=50 mm/min, geometry B

The stress intensity factor, K_I, expresses stress concentration at the crack tip caused by an applied load. When K_I exceeds the material toughness ($K_I \geq K_{IC}$), crack propagation occurs. Test curves show that after the maximum force (σ_{eng}) has been reached, a rapid stress reduction follows as the crack propagates through the specimen. This decreasing phenomenon ends with the specimen rupture; crack grows self-similarly and cuts the binder ligaments without them being significantly stretched before rupture. K_{IC} is a material property just like the strength only if it is independent from the specimen geometry. Evidence for K_{IC} geometry independence is provided in Figure 8. There is no thickness effect, i.e. K_{IC} is constant with thickness. Instead, K_{IC} depends on strain rate. Figure 9 shows that the dependence of K_{IC} on strain rate is parabolic, this trend is in agreement with literature studies[6] and Shapery's general fracture theory[7] for viscoelastic materials. Physically, this growth is due to the higher amount of mechanical energy dissipated through viscous relaxation. Moreover, this graph shows a similar crack propagation behavior for propellants B and C; propellant B displays a slightly lower toughness value. A possible explanation can be related to its chemical composition; in fact, propellant B contains coarser AP. These large grains act as stress concentrators for the binder, enhancing propagation.

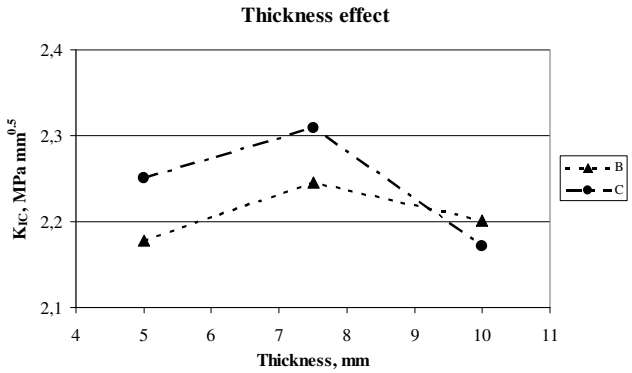

Figure 8 : Thickness effect on toughness

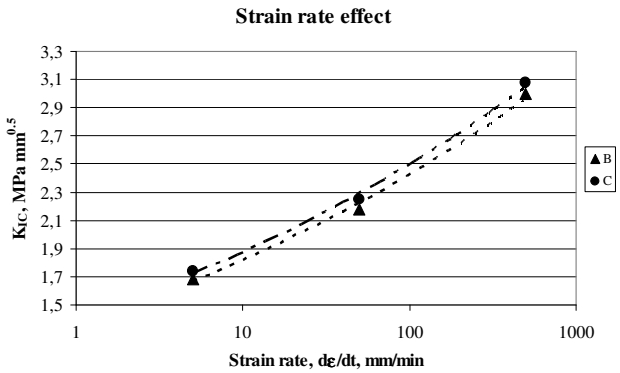

Figure 9 : Strain rate effects on toughness

Elastic materials loaded with a stress step react immediately with a strain step. Viscous material, instead, give a delayed, increasing strain until the reaching of the rupture strain. Viscoelastic materials show an initial response related elastic behavior, then an increasing strain due to the viscous part. When the crack propagation occurs, the

viscous effect leads to an exponential law for the crack velocity: $da/dt=bK_I^n$. The exponent value can be determined knowing the applied load and the instantaneous crack dimension during tensile test. Through interpolation in a bilogarithmic graph, *b* and *n* can be evaluated. Crack propagation (da/dt) is calculated as a fraction of the shorter ligament length and the time interval occurred between the reaching of the ultimate strength and specimen rupture. The propellants interpolating lines are characterized by different slopes. Crack growth in propellant C propagates at a higher velocity than in propellant B ($n_B = 4.4988$; $n_C = 5.5159$).

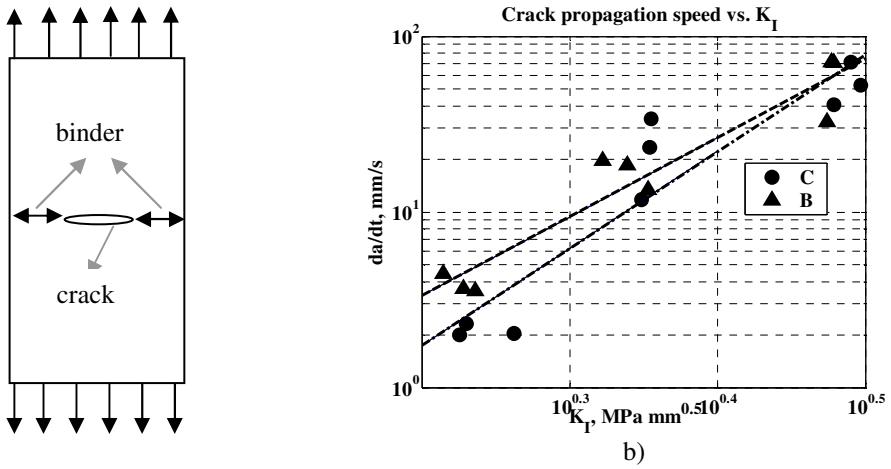

Figure 10 : a) Scheme of the tensile test of a MT specimen b) Crack propagation speed vs. K_I

4. Burning rate augmentation effects

A close observation of the investigated propellant formulations using an optical microscope, shows that the primary factor influencing the toughness is the effectiveness of the bonding agent, a molecule generating strong bonds between the inorganic oxidizer grains and the binder. In absence of a good bonding agent, dewetting occurs at low strain and the AP particles act like voids in the binder. In particular, self-produced formulations without bonding agent, but having the same AP/Al/HTPB/curing agent/plasticizer content than the described industrial formulations B and C, proved to be very brittle, unlike B and C.
Propellants without bonding agent readily display dewetting-induced microcracks upon straining. Micro-crack formation, nucleation and propagation occurs continuously upon strain application. On the contrary, industrial propellants do not exhibit any cavitation until a threshold strain is reached, upon which there is either a dewetting of AP particles from the binder (limited bonding agent effectiveness), or microcrack formation at spots of local stress concentration, near large oxidizer grains (effective bonding agent), or a combination of both phenomena.

The bonding agent and its effectiveness also influence the steady burning rate properties of all formulations[8--10]. In particular, if the material is damaged and microcracks are formed, the application of a tensile load, like in the propellant layer near the bore surface of a solid rocket motor (SRM) when the latter is cooled below curing temperature, keeps the microcracks open. As a consequence, thermal energy feedback from the flame into the material is enhanced; in particular, at low pressure and in absence of convection and radiation, conduction can ignite the propellant inside the cracks. In a motor, the high levels of convection and radiation enhance thermal energy feedback into the now porous material. The increased thermal power transmitted to the solid generates a higher burning rate.
The agent through which the burning rate augmentation effect due to strain and tensile load application occurs is the onset of microcracks in the material (i.e. the onset of dewetting or cohesive microcrack formation in the binder), as suggested by Summerfield[11]. His hypothesis was confirmed by a series of dedicated experiments[9,10], which show the magnitude of the burning rate augmentation effect. Accurate modeling is reported in Margolis and Williams[12].
For the industrial formulations described above, no burning rate augmentation effect is expected at a strain below the onset of dewetting, i.e. at about 15% strain at 50 mm/min and room temperature. For brittle formulations containing no bonding agent, or for which the bonding agent is not effective, the augmentation effect occurs proportionally to the applied strain.
This mechanism is expected to generate a measurable scale effect between thick-walled development motors and flight-weight hardware, and between new and aged motors. Safety issues arise if the pressure sensitivity of oxidizer and propellant are high, such as in new energetic materials formulations under development, containing energetic

binder and plasticizer or oxidizers which are less stable than AP. Several authors[13-15] showed that deflagration in a porous material can evolve in a detonation.

4. Conclusions

A mechanical characterization of four composite solid propellants based on AP/HTPB/Al showed the important effect of the oxidizer grains size and their distribution on classic and fracture mechanical failure properties. The latter have been measured in terms of the toughness at different strain rates, using MT specimens of different thickness; the thickness effect proved to be negligible, as expected.
This test technique gave reproducible results, in good agreement with Shapery's general theory on the fracture mechanics of viscoelastic particulate composites. Its application to complete the mechanical characterization of any composite propellant during development or production would provide essential information to assess the safety of solid rocket motors at ignition, particularly those showing flaws after manufacturing or part of their service life.

References

[1] Chang, I.S., Patel, N.R. and Yang, S. Titan IV Motor Failure and Redesign Analyses, *Journal of Spacecraft and Rockets*, 32:4:612-618, 1995.
[2] AGARD. Structural Assessment of Solid Propellant Grains. *Agard Advisory Report 350, Propulsion and Energetic Panel*, North Atlantic Treaty Organization, Neuilly-Sur-Seine, France, December 1997.
[3] Brunella, G.B. Caratterizzazione meccanica di propellenti solidi compositi. Master Thesis in Aeronautical Engineer, SPLab, Energy Department, Politecnico di Milano, December 2006.
[4] An. STANAG 4506. Explosive Materials, Physical /Mechanical Properties, Uniaxial Tensile Test. *Military Agency for Standardization*, NATO, March 2000.
[5] An. ASTM-E-647-05. Standard Test Method for Measurement of Fatigue Crack Growth Rates. *ASTM International*, 2005.
[6] Sandri Tussiwand, G., Saouma, V.E., DeLuca, L.T. and Terzenbach, R. Fracture Mechanics of Composite Solid Rocket Propellant Grains, Part I: Material Testing. Paper submitted for publication to the *AIAA Journal of Propulsion and Power*, April 2007.
[7] Shapery, R.A. A theory of crack initiation and growth in viscoleastic media. Part II. *International Journal of Fracture*, 11:3:369-388, 1975.
[8] Sandri Tussiwand, G. Structural ballistic interaction effects on composite solid propellants and rocket motors. PhD. Thesis, Politecnico di Milano, Dipartimento di Ingegneria Aerospaziale, June 2007.
[9] Sandri Tussiwand, G., Maggi, F., Bandera, A. and DeLuca, L.T. Intrinsic structural-ballistic interactions in composite energetic material. Part I- Experiments., *International Conference on Non-Isothermal Phenomena and Processes*, 27th November-1st December 2006, Yerevan, Armenia.
[10] Sandri Tussiwand, G., Maggi, F., Bandera, A. and DeLuca, L.T. Intrinsic structural-ballistic interactions in composite energetic material. Part II- Modelling. *International Conference on Non-Isothermal Phenomena and Processes*, 27th November-1st December 2006, Yerevan, Armenia.
[11] Summerfield, M. and Parker, K.H. Interrelations between combustion phenomena and mechanical properties in solid propellant rocket motor. Mechanics and Chemistry of Solid Propellants. Eringen, A.C., editor, Pergamon Press, Oxford, 1967.
[12] Margolis, S.B. and Williams, F.A. Structure and Stability of Deflagrations in Porous Energetic Materials. SANDIA Report SAND-99-8453, New Mexico, USA, 1999.
[13] Kuo, K.K. and Kooker, D.E. Coupling Between Nonsteady Burning and Structural Mechanics of Solid Propellant Grains. In Nonsteady Burning and Combustion Stability of Solid Propellants, in *AIAA Progress in Astronautics and Aeronautics Series*, Vol. 143, DeLuca, Price and Summerfield editors, 1992.
[14] Krier, H. and Gokhale, S.S. Modeling of Convective Mode Combustion through Granulated Propellant to Predict Detonation Transition. *AIAA Journal*, 16:2:177-183, February 1978.
[15] Mellor, A.M., Boggs, T.L., Covino, J., Dickinson, W., Dreitzler, D., Thom, L.B., Frey, R.B., Gibson, W., Roe, W.E., Kirshenbaum, M. and Mann, D.M. Hazard Initiation in Solid Rocket and Gun Propellants and Explosives. *Prog. Energy Combust. Sci,* 1988, 14:213-244, Pergamon Press, 1989.

This page has been purposedly left blank